

Supporting Information

Graphene nanobubbles on TiO₂ for *in operando* electron spectroscopy of liquid-phase chemistry

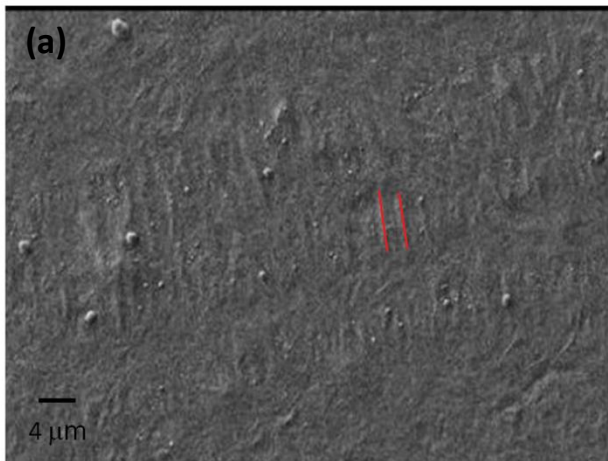
S. Nappini^{†*}, *A. Matruglio*^{#†}, *D. Naumenko*[†], *S. Dal Zilio*[†], *F. Bondino*[†], *M. Lazzarino*[†], *E. Magnano*^{† § *}

[†] IOM-CNR, Laboratorio TASC, S.S. 14-km 163.5, 34149 Basovizza, Trieste, Italy,

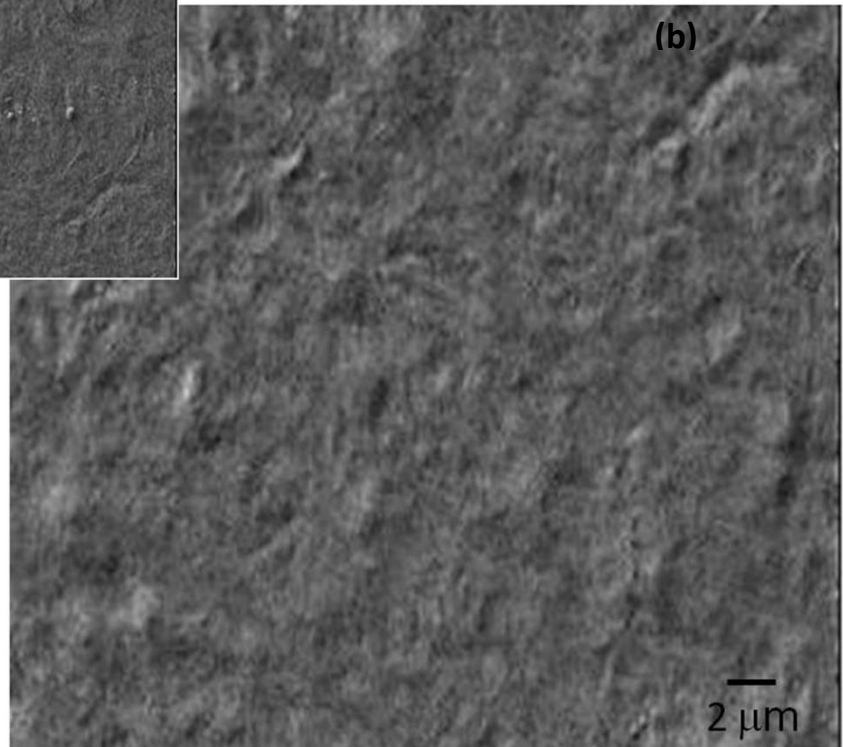
[#] University of Trieste, Graduate School of Nanotechnology, Piazzale Europa 1, 34127 Trieste, Italy,

[§] Department of Physics, University of Johannesburg, PO Box 524, Auckland Park, 2006, Johannesburg, South Africa

SEM



← **Wrinkles:** stripes aligned along one preferential direction

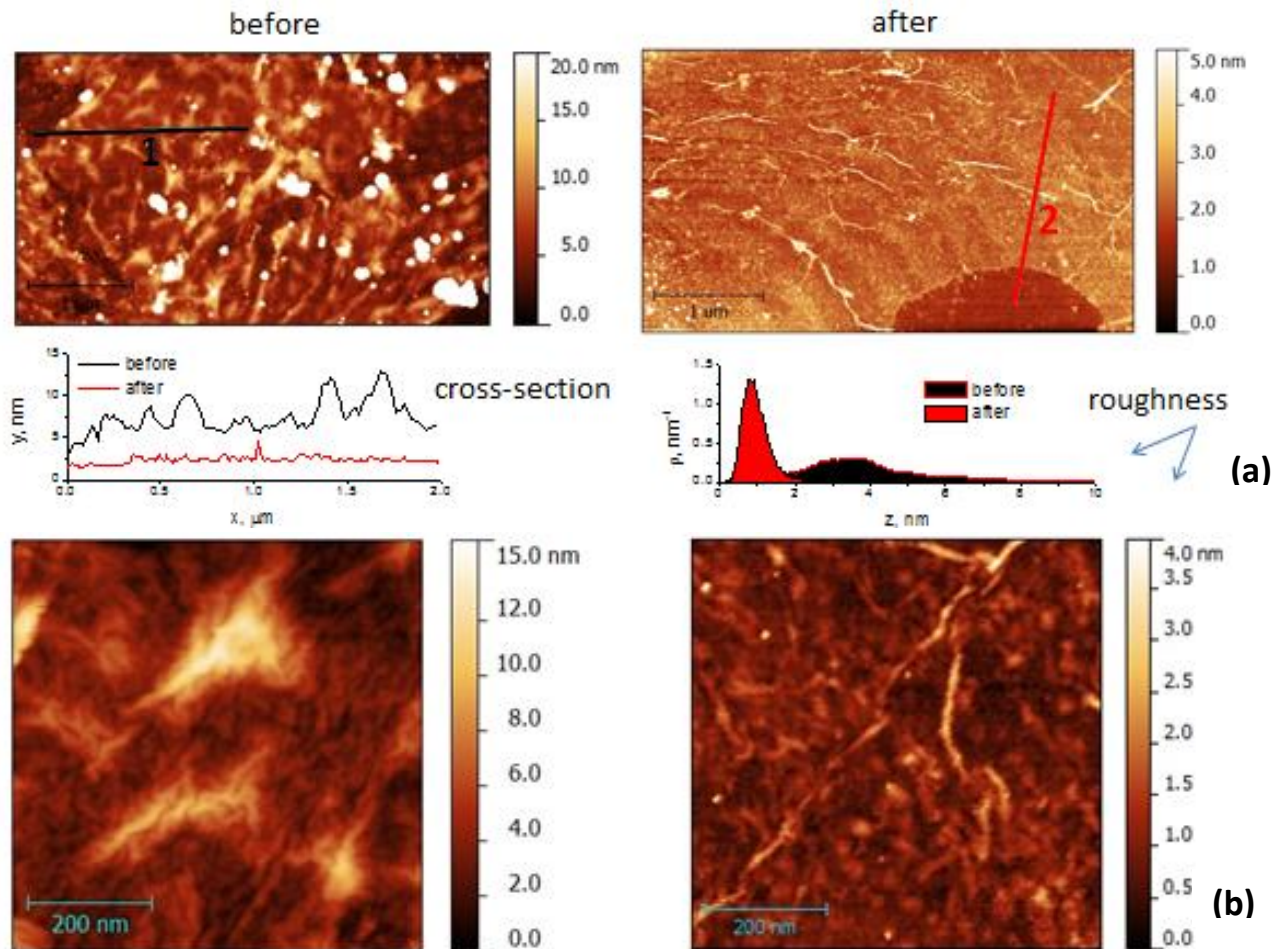


Nanobubbles: irregularly shaped vesicles of different size which range from few hundreds nanometers to few micrometers

S1. SEM pictures of Gr transferred on a TiO₂ crystal on two different regions: (a) area with wrinkles, (b) area with a high density of graphene nanobubbles.

Graphene nanobubbles have irregular shape and different size ranging from hundreds nanometers to few micrometers, while graphene wrinkles are stripes aligned along a preferential direction which depends to the interaction between graphene and substrate.

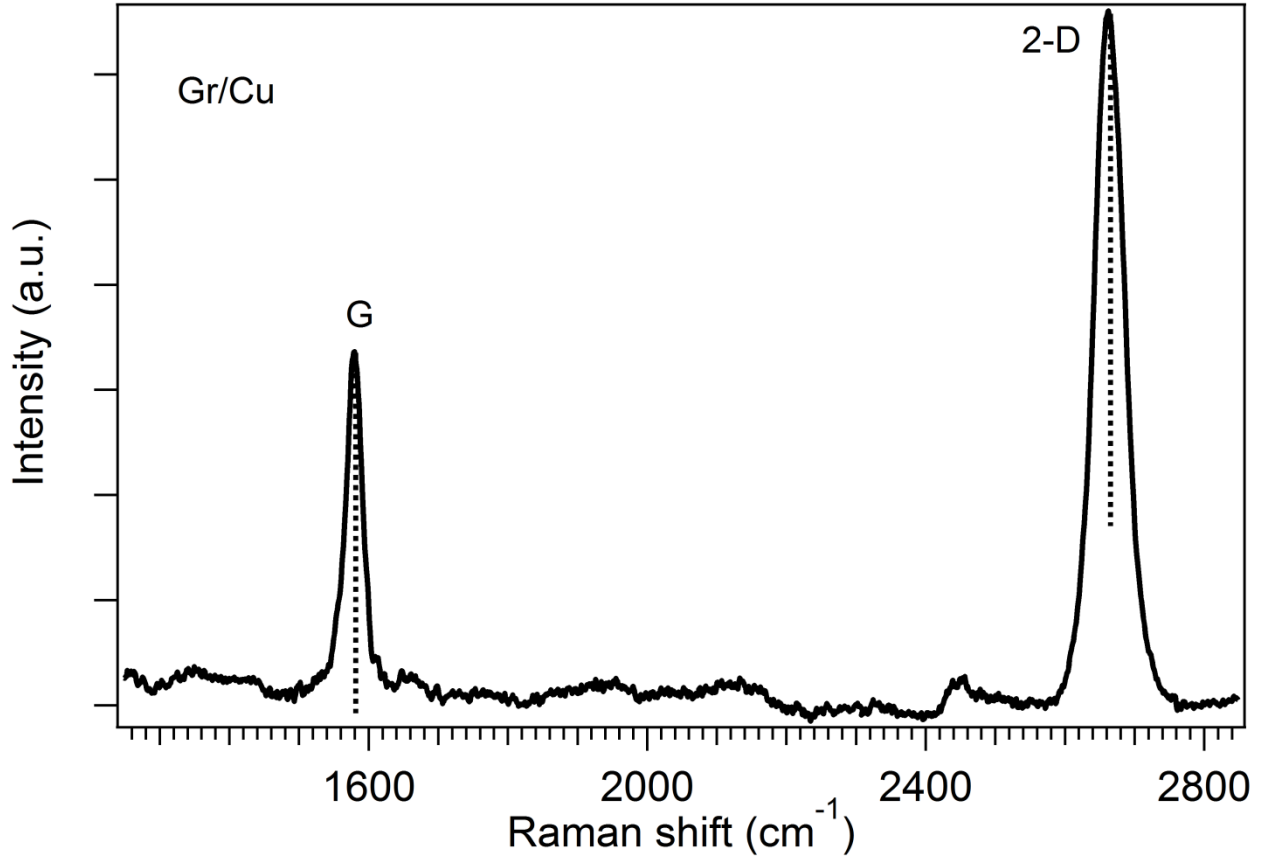
AFM



S2. (a) AFM pictures of Gr transferred on a TiO₂ crystal (scale bar 1 μm) before (on the left) and after the annealing (on the right). A contamination by polymer residues can be seen on Gr surface that is vanished after annealing in UHV. The Gr surface roughness is reduced from 3.5 nm to 1 nm testifying the formation of flat Gr after the annealing.

(b) AFM pictures in a zoomed area (scale bar 200 nm) before (on the left) and after the annealing (on the right).

RAMAN



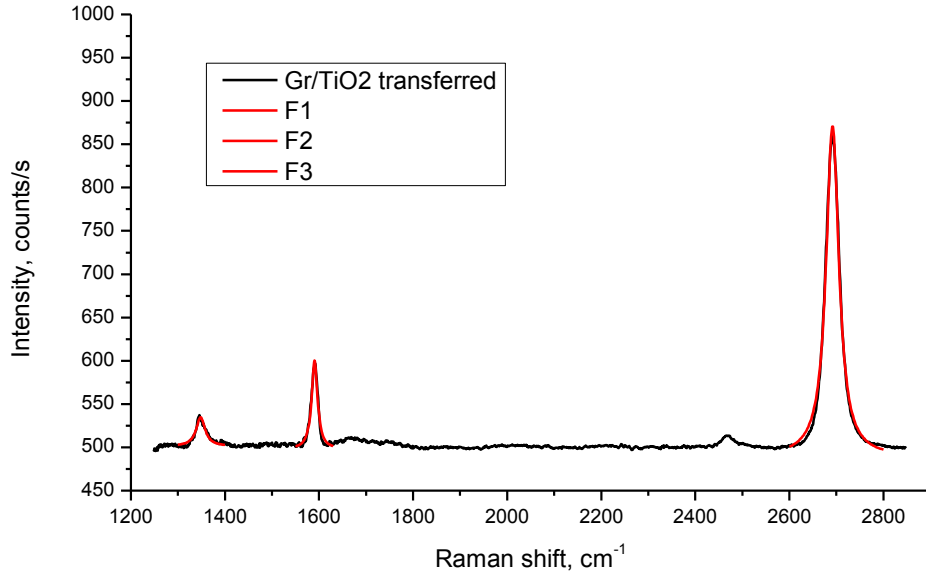
S3. Raman spectra of commercial as-grown Gr acquired directly on Cu foil before the transfer. The excitation wavelength is 532 nm; the laser power on the sample is 1 mW. No distinguishable D peak is observed providing an indication of the good quality of this sample.

CALCULATION OF THE STRAIN

Fit function:

$$y = y_0 + \frac{2A}{\pi} \frac{w}{4(x - x_c)^2 + w^2}, \quad H = \frac{2A}{\pi w} \quad (1)$$

	transferred			annealed		
	D	G	2D	D	G	2D
x_c	1348.2	1590.6	2691.9	1352.2	1595.0	2701.7
w	22.8	15.1	32.6	40.2	26.7	43.3
A	1203.6	2430.7	19624.5	2447.8	6957.4	14473.1
H	33.5	102.6	383.0	38.7	165.8	212.8



Example of the D peak, G peak, and 2D peak fittings with Lorentzian function (1).

The equation to calculate the strain ε is [1]:

$$\varepsilon = \frac{\Delta\omega}{2\gamma\omega_0}$$

where γ is the Gruneisen parameter taken from the ref [1], $\Delta\omega = \omega_1 - \omega_2$ is the Raman frequencies shift between compressive and tensile, respectively and $\omega_0 = \frac{1}{2}(\omega_1 + \omega_2)$

For the D, G, and 2D peaks:

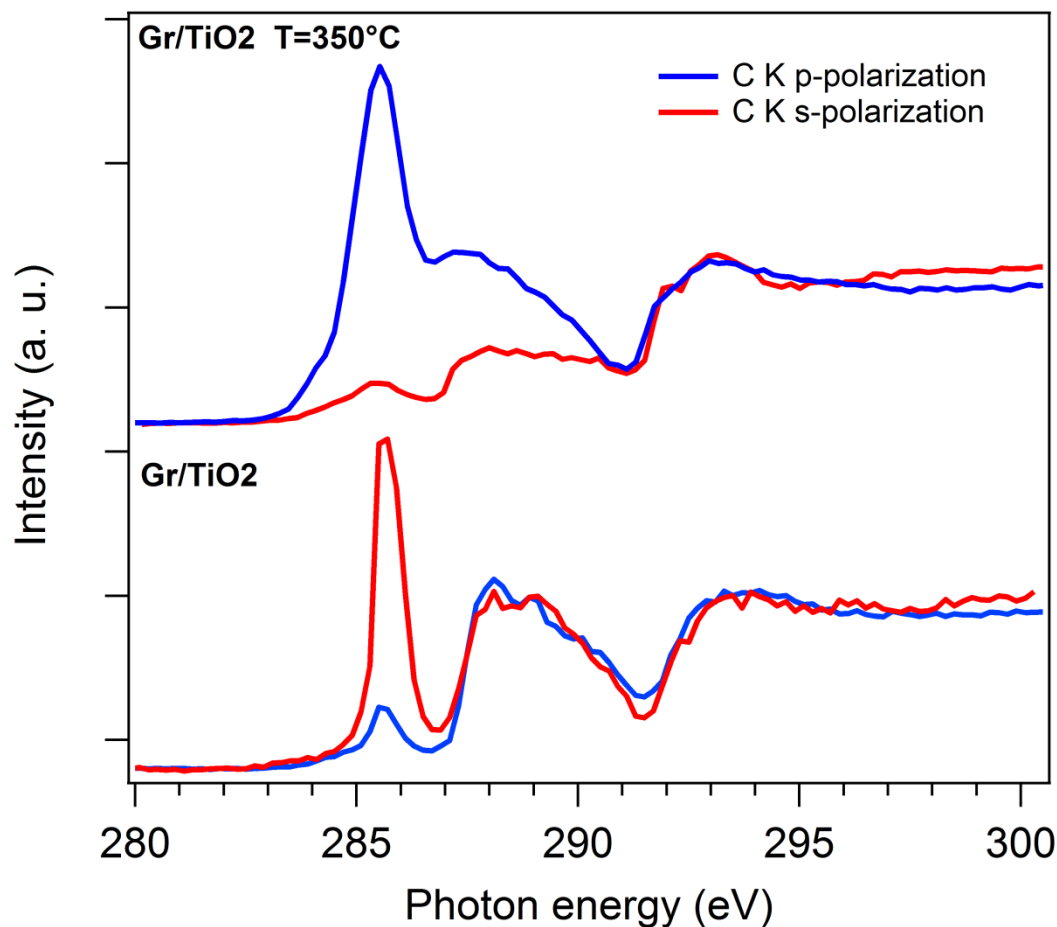
$$\varepsilon_D = \frac{4}{2 \cdot 2.52 \cdot 1348.2} = 5.9 \cdot 10^{-4}; \quad \varepsilon_G = \frac{4.4}{2 \cdot 1.8 \cdot 1590.6} = 7.7 \cdot 10^{-4}; \quad \varepsilon_{2D} = \frac{9.8}{2 \cdot 2.6 \cdot 2691.9} = 7 \cdot 10^{-4};$$

Averaged strain:

$$\varepsilon = (0.069 \pm 0.009)\%$$

[1] Zabel, J., Nair, R.R., Ott, A., Georgiou, T., Geim, A.K., Novoselov, K.S., Casiraghi, C. Raman spectroscopy of graphene and bilayer under biaxial strain: Bubbles and balloons (2012) Nano Letters, 12 (2), pp. 617-621.

C K-edge NEXAFS

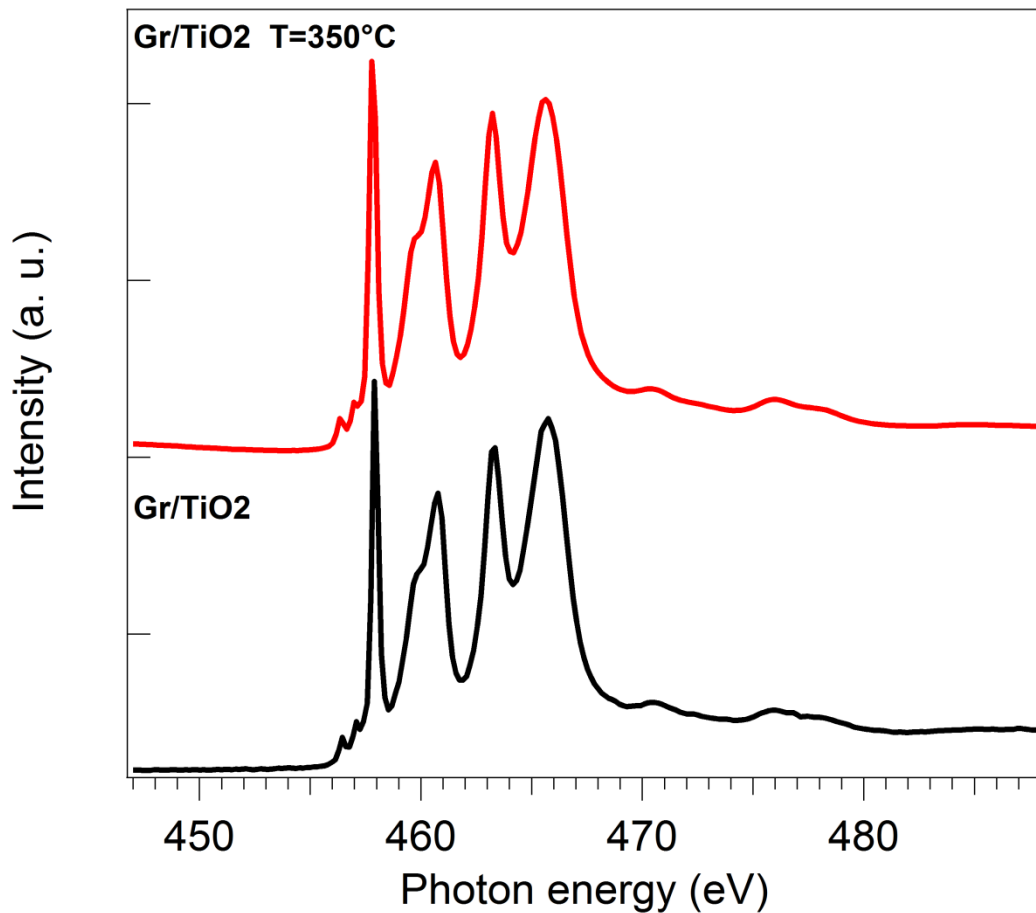


S4. Polarization dependent NEXAFS at C-K edge of as-transferred Gr/TiO₂ (lower part) and Gr/TiO₂ annealed at 350°C in UHV (upper part).

In the sample annealed at 350°C a strong feature at 284 eV and a weak one at 285 eV in the $1s \rightarrow \pi^*$ region can be associated to the transition of C $1s$ core electrons to two unoccupied C-Ti hybridized states. A pronounced polarization dependence, shown by the suppression of π^* states with s-polarized light, clearly shows that the Gr sheet is nearly flat.

C K-edge spectra of as-transferred Gr show a limited dichroism of the π - and σ -resonances in comparison to annealed Gr. This behavior can be observed in systems with curved morphology, where the orientation of the π^* orbitals with respect to the electrical polarization changes continuously along the surface.

XAS Ti L_{2,3}-edge



S5. XAS at Ti L_{2,3} edge of rutile in as-transferred Gr/TiO₂ (black curve) and Gr/TiO₂ annealed at 350°C in UHV (red curve). The spectra are identical.

Both Ti L_{2,3} XAS spectra clearly show the typical structure of rutile single crystal [2] with two small pre-edge features at 456.4 eV and 457 eV, and the distinctive splitting of the L₂ and L₃ components into two doublets namely the t_{2g} and e_g sublevels, due to octahedral (O_h) crystal field. In the L₃ component, three lines can be identified: the empty Ti 3d states with a t_{2g} symmetry (457.9 eV), and 3d states with e_g symmetry (459.8 and 460.8 eV)

In the L₂ region, only two lines can be identified at 463.3 eV and 465.7 eV due to the stronger t_{2g} and e_g overlap. Satellite structures at higher photon energy are also present.

Ti L_{2,3} XAS show that the stoichiometry of TiO₂ crystal is not affected by the presence of Gr, and confirm its resistance to chemical and thermal treatments during the transfer procedure.

[2] Mosquera, A. A.; Endrino, J. L.; Albella, J. M. *J. Anal. At. Spectrom.* **2014**, 29 (4), 736–742.

XAS Fe and Cu L_{2,3}-edge

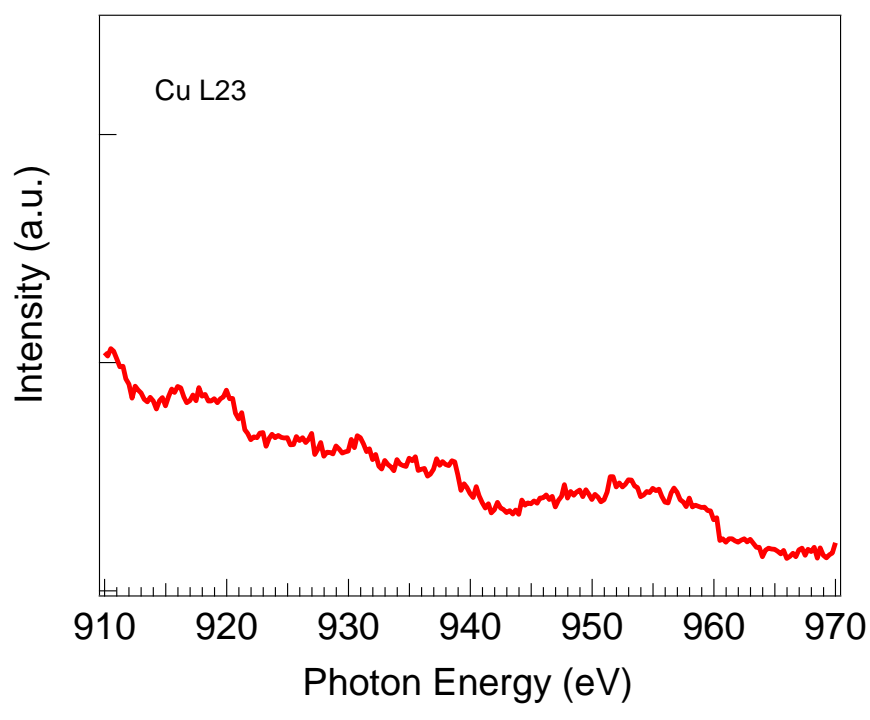
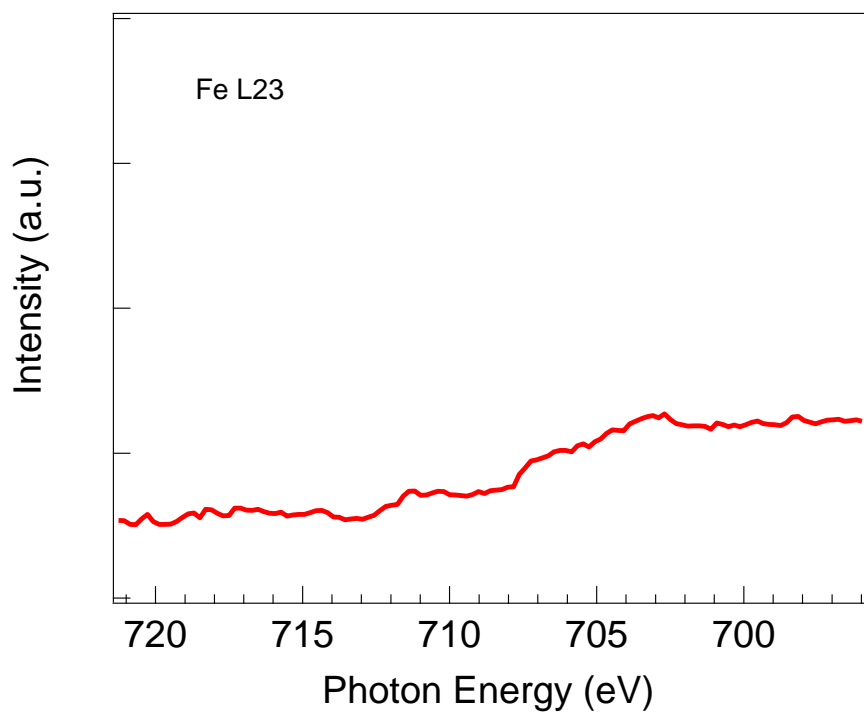
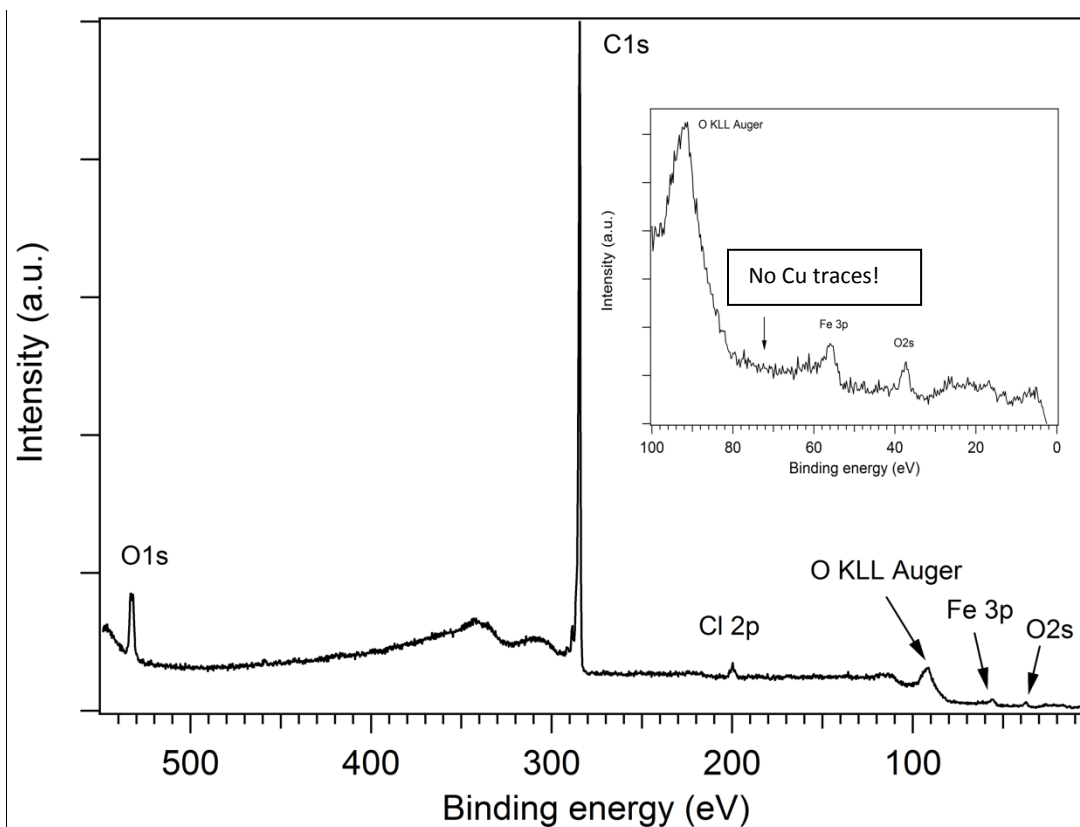


Figure S6. XAS spectra at the L_{2,3} edge of Fe (a) and Cu (b).

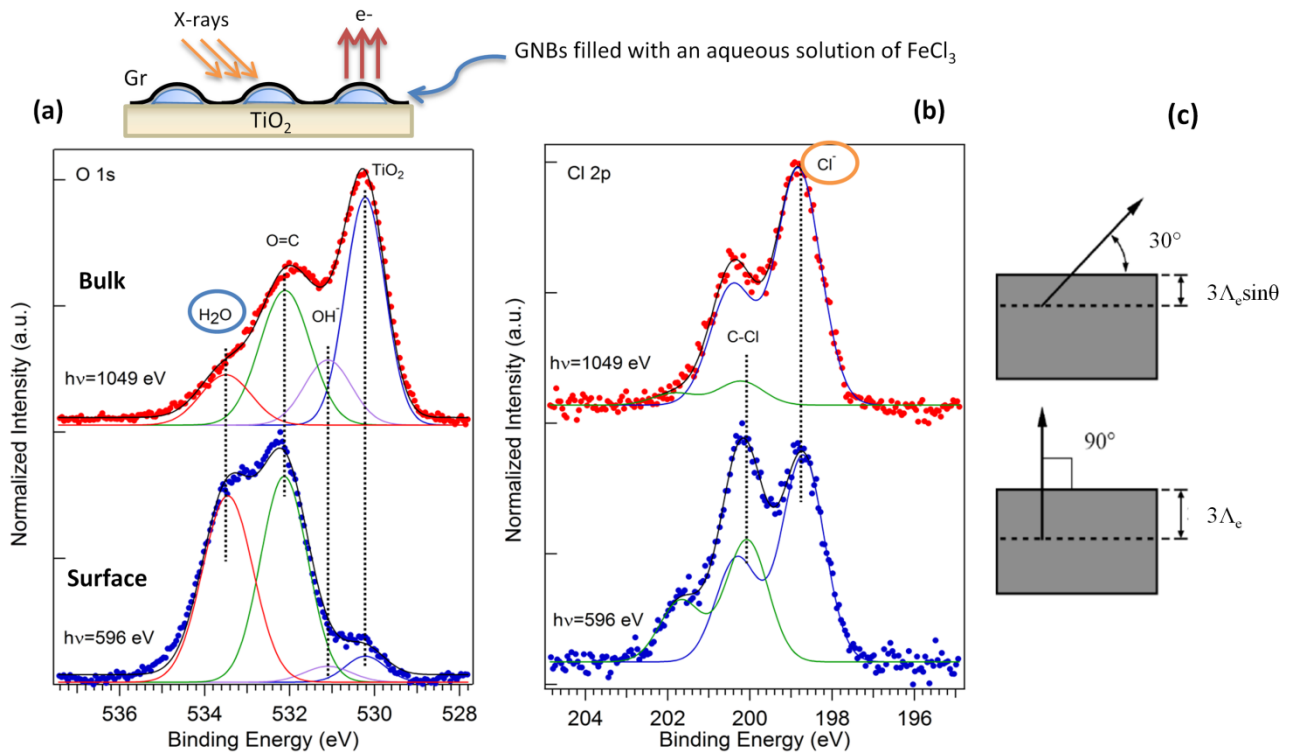
No contamination due to Fe from the FeCl₃ etching solution or Cu residuals from copper foil are detectable.

Survey of FeCl₃ samples encased in GNBs



S7. Survey spectrum recorded at 596 eV of photon energy. No traces of Cu contaminants are visible from XPS measurements. The concentration of Cu residues dissolved in solution is estimated to be 1800 times lower than FeCl₃ concentration. No effects induced by copper in the thermal reduction of FeCl₃ are expected due to the extremely low Cu content.

XPS O1s and Cl 2p of FeCl₃ solution at different photon energies

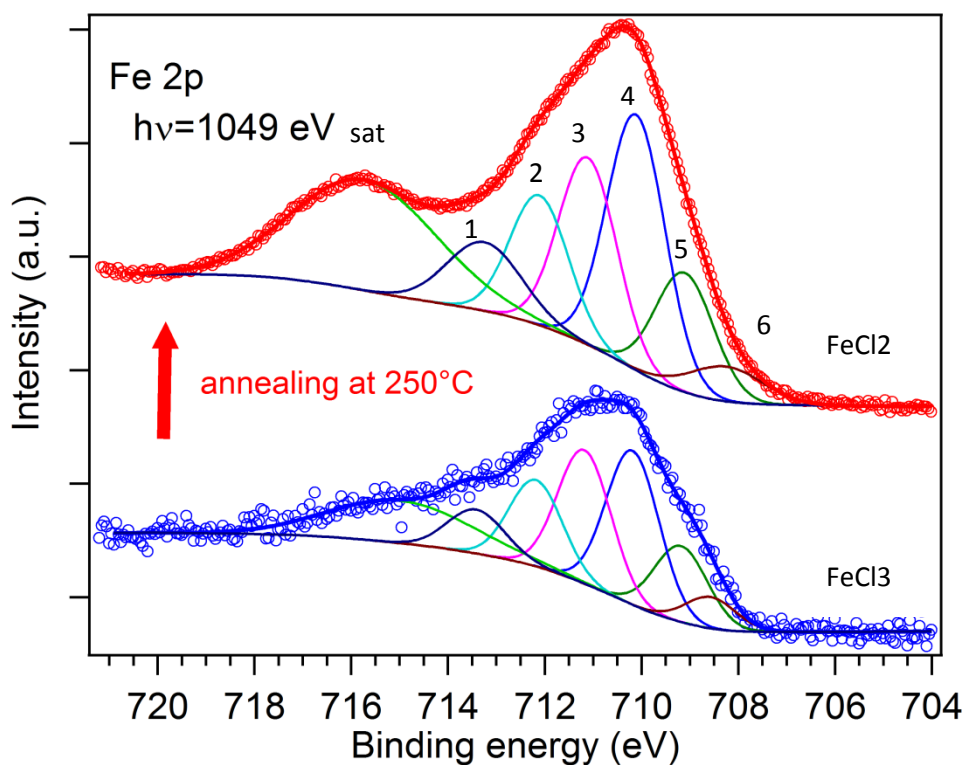


S8. (a) O1s and (b) Cl 2p XPS spectra of GNBs filled with an aqueous solution of FeCl₃ (1.6 M) acquired at normal emission geometry (see scheme in figure c) using a surface-sensitive photon of 596 eV in energy (blue curve) and a more bulk sensitive photon of 1049 eV in energy (red curve). (c) A scheme of different configurations adopted for XPS acquisition: grazing emission geometry (surface sensitive, on the top), and normal emission geometry (bulk sensitive, on the bottom).

The position of the sample at 1049 eV and 596 eV could be slightly different.

FeCl₃ SOLUTION BEFORE AND AFTER ANNEALING

XPS Fe 2p_{3/2}

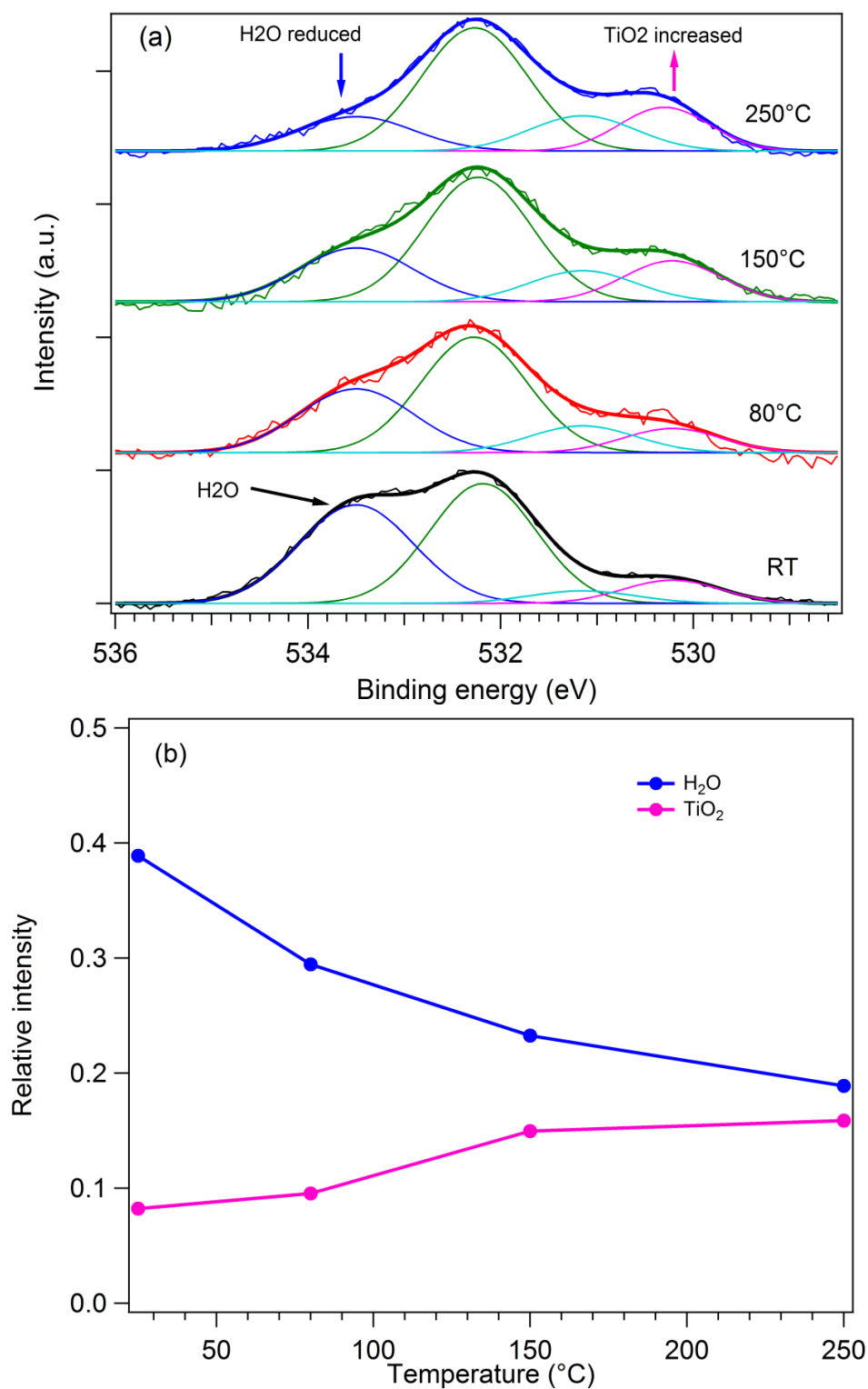


S9. XPS spectra at the 2p_{3/2} edge of Fe before and after the annealing.

The spectra and the corresponding fitting components are in good agreement with those reported in literature [3]

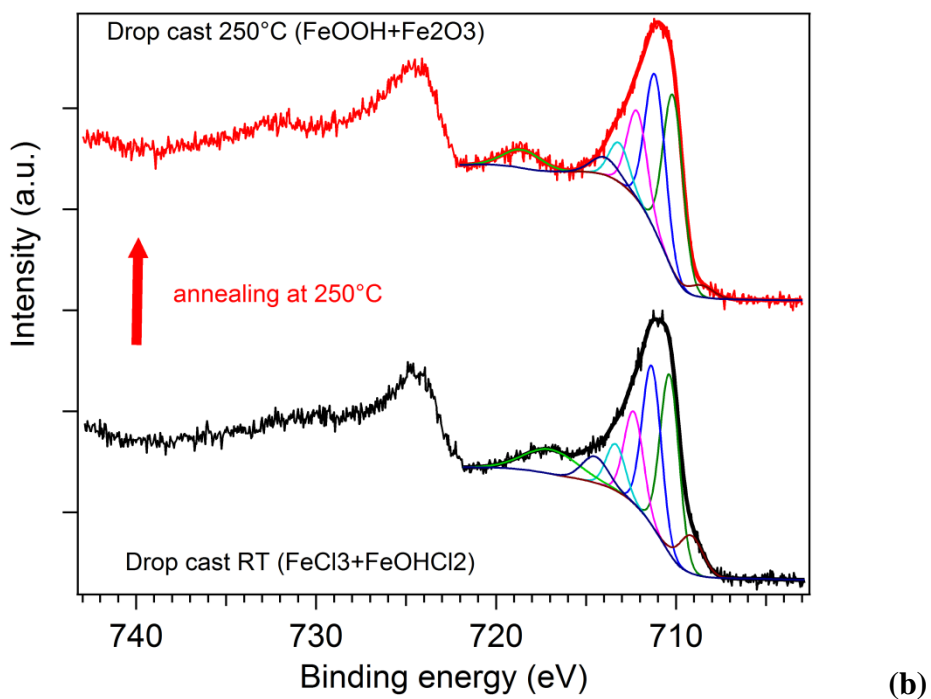
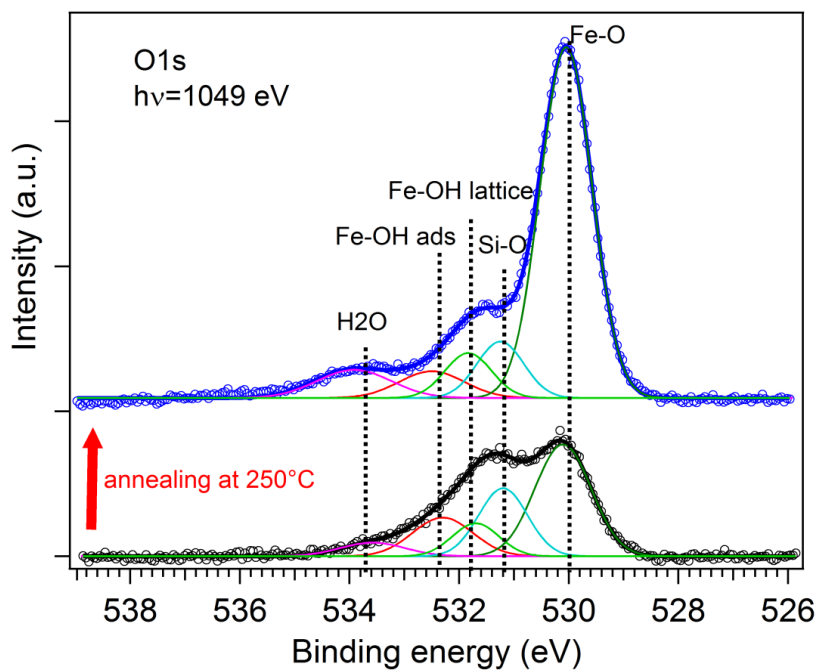
[3] Grosvenor, A. P.; Kobe, B. A.; Biesinger, M. C.; McIntyre, N. S. *Surf. Interface Anal.* **2004**, 36 (12), 1564–1574.

XPS O1s after annealing at 80°C



S10. (a) XPS spectra of O1s from RT to 250°C recorded at normal emission geometry. The water component is still present even after the annealing. (b) Evolution of H₂O and TiO₂ components as function of the annealing temperature.

FeCl₃ DROP CAST



S11. O 1s (a) and Fe 2p (b) spectra before and after the annealing at 250°C.

Spectra before annealing are consistent with those of FeCl₃ or FeOHCl₂ [3,4], while those after annealing correspond to Fe₂O₃ or FeOOH [4,5].

[4] Y. J. Kim and C. R. Park, *Inorganic Chemistry*, Vol. 41, No. 24, 2002

[5] J. Baltrusaitis, D. M. Cwiertnya and V. H. Grassian, *Phys. Chem. Chem. Phys.*, 2007, 9, 5542–5554